

Asymmetry of $\vec{p} + \vec{p} \rightarrow \gamma + jet + X$ process and problem of ΔG

G.P.Škoro¹,

*Faculty of Physics, University of Belgrade,
Institute of Nuclear Sciences "Vinča",
Belgrade, Yugoslavia*

M.V.Tokarev²

*Laboratory of High Energies,
Joint Institute for Nuclear Research,
141980, Dubna, Moscow Region, Russia*

Abstract

The $\gamma + jet$ production in $\vec{p}-\vec{p}$ collisions at high energies is studied. Double-spin asymmetry A_{LL} of the process is calculated by using Monte Carlo code SPHINX. The predictions for A_{LL} of the $\gamma + jet$ production in the $\vec{p}-\vec{p}$ collisions using the spin-dependent gluon distributions with positive and negative sign of $\Delta G(x, Q^2)$ are made at RHIC energies. A possibility to extract the spin-dependent gluon distribution $\Delta G(x)$ at STAR experiment and to discriminate between different theoretical scenarios is discussed.

¹goran@rudjer.ff.bg.ac.yu

²tokarev@sunhe.jinr.ru

1 Introduction

The accelerator complex of polarized protons (RHIC-spin) at Brookhaven National Laboratory will be first proton-proton collider accelerating proton beam up to energy of 250 GeV with polarization $\simeq 70\%$ and luminosity up to $L \simeq 2 \cdot 10^{32} \text{ cm}^{-2}\text{s}^{-1}$ at $\sqrt{s} = 500 \text{ GeV}$. RHIC-spin will have unique capability to study polarization phenomena such as direct γ , jet, dijet, Drell-Yan lepton pairs and W^\pm, Z^0 [1, 2, 3] production and to perform the test of perturbative and non-perturbative QCD. The main goal is to obtain direct information on the spin-dependent gluon and sea quark distribution and to clarify nature of proton spin.

In our previous works [4, 5], we studied the double-spin asymmetry A_{LL} of jet, dijet and direct- γ production in $\vec{p} - \vec{p}$ collisions at RHIC energies as a function of sign and shape of spin-dependent gluon distribution ΔG and made predictions of A_{LL} for the STAR experiment planed at RHIC [3, 6]. We would like to note that global fits [7] to the present inclusive DIS data cannot even fix the sign of ΔG , not mentioning its magnitude [8]. For example, one of the analysis [9] favors a positive sign, while the recent NLO analysis [10] yields negative first moment of the gluon density. Both positive and negative values of the sign of $\Delta G(x, Q^2)$ over a wide kinematic range ($10^{-3} < x < 1$) were considered in [11]. The possibility to draw conclusions on the sign of the spin-dependent gluon distribution, $\Delta G(x, Q^2)$, from existing polarized DIS data have been studied in [12]. The result of the DIS data analysis [12] on g_1^n supports the conclusion that the sign of $\Delta G(x, Q^2)$ should be positive. Also, the recent HERMES result [13] indicates that $\Delta G/G$ is positive in the intermediate x region. Nevertheless, the additional confirmations on sign of ΔG are required and the experiments for direct measuring of the $\Delta G/G$ are necessary. We also consider that the NLO QCD analysis with negative sign of $\Delta G(x, Q^2)$ of DIS data on g_1 structure function could give additional constraints of quark and gluon distributions moreover usually used [7].

The measurement of the $\gamma + jet$ production in polarized proton-proton collisions is more perspective for determining $\Delta G(x)$ because the reaction is dominated by the Compton $qq \rightarrow \gamma q$ scattering and we can assume that $\Delta q(x)/q(x)$ is known from polarized DIS experiments [15]-[22]. Some contributions to the cross section of $\gamma + jet$ production come from non-direct mechanisms such as $\bar{q}q$ annihilation, photon fragmentation and k_\perp smearing³.

The main goal of this work is to made predictions of double-spin asymmetry A_{LL} of the $\vec{p} + \vec{p} \rightarrow \gamma + jet + X$ process and to study the possibility of direct extraction of spin dependent gluon distribution $\Delta G(x)$ from this reaction at STAR detector at RHIC. The determination of ΔG by means of $\gamma + jet$ asymmetry is connected with large background, similar as in the case of prompt photon production. Two closely spaced photons resulting from decay of high p_T neutral mesons (π^0, η) can produce fake 'direct photon signal' in detector. Because the cross-sections of the main subprocesses for 'direct' mesons production in the pp collision ($qq \rightarrow qq, qg \rightarrow qg, gg \rightarrow gg$) are much higher than the cross-section for Compton scattering, we can expect the large yield of background (direct meson + jet) events. So, the additional aim of the present paper is to study the

³The discussion on the problem can be found in [3] and references therein.

kinematic properties of signal (S) and background (B) and to find the corresponding algorithm for background reduction.

The paper is organized as follows. The different sets of spin-dependent parton distributions used in Monte Carlo (MC) simulations are described in Section 2. The procedure for calculation of A_{LL} and extraction of $\Delta G(x)$, together with the results of MC simulations at $\sqrt{s} = 200 \text{ GeV}$ are given in Section 3. Conclusions are summarized in Section 4.

2 Spin-dependent gluon distribution

The 3 sets of spin-dependent parton distributions [11] and [14] are used to calculate the $\gamma + jet$ asymmetry A_{LL} . First set is based on work of Altarelli and Stirling [14] and include a scenario with large gluon polarization ΔG . Second and third ones have been obtained by the phenomenological method [11] including some constraints on the signs of valence and sea quark distributions, taking into account the axial gluon anomaly and utilizes results on integral quark contributions to the nucleon spin. Based on the analysis of experimental data on deep inelastic structure function g_1 the parameterization of spin-dependent parton distributions for both positive and negative sign of ΔG have been constructed. It was found that the Q^2 evolution of structure function g_1 is sensitive to sign of ΔG . We would like to note the both sets of distributions describe experimental data very reasonable. We shall denote $\Delta G^{>0}$ and $\Delta G^{<0}$ sets of spin-dependent parton distributions obtained in [11] with positive and negative sign of ΔG , respectively. It was shown in [23] that phenomenological method reproduces the main features of the NLO QCD Q^2 -evolution of proton, deuteron and neutron structure function g_1 . Therefore the constructed spin-dependent quark and gluon distributions can be reasonably used to study the asymmetry A_{LL} of $\gamma + jet$ production in $\vec{p} - \vec{p}$ collisions too.

Figure 1(a) shows the dependence of the ratio $\Delta G(x, Q^2)/G(x, Q^2)$ on x at $Q^2 = 50 \text{ (GeV)}^2$ for gluon distributions [14] and $\Delta G^{>0}$ [11]. The curve [14] increases with x and then decreases to zero. The behavior is due to the structure of the ratio $\Delta G/G \sim x^\alpha(1-x)^\beta$. The monotonous increase of an second curve with x connects to other asymptotic of the ratio $\Delta G/G \sim x^\delta$ at $x \rightarrow 1$. Figure 1(b) shows the dependence of the ratio $\Delta G(x, Q^2)/G(x, Q^2)$ on x at $Q^2 = 50 \text{ (GeV)}^2$ for gluon distributions $\Delta G^{>0}$ and $\Delta G^{<0}$ [11].

The integral contributions of gluons $\Delta g(Q^2) = \int_0^1 \Delta G(x, Q^2) dx$ to the proton's spin are found to be $\Delta g^{>0} \simeq 2$, $\Delta g^{<0} \simeq -3.4$ at $Q^2 = 10 \text{ (GeV)}^2$ [11], and $\Delta g \simeq 3$ at $Q^2 = 10 \text{ (GeV)}^2$ [14]. Because integral quark contributions to the proton's spin is practically the same for all the parameterizations, the difference in asymmetry A_{LL} should reflects the difference in shape of gluon distribution (and sign of ΔG) used. We would like to note that large value of gluon polarization corresponds to relatively small contribution of $q\bar{q} \rightarrow g\gamma$ process to the final $\gamma + jet$ asymmetry. Because this process has the same final state as a signal, it is the background for determining the ΔG . But, our calculations shows that, at RHIC energies, the cross-section for $q\bar{q} \rightarrow g\gamma$ process is practically for an order of magnitude smaller than the cross-section for $qg \rightarrow \gamma q$ process, for all spin-dependent PDF's used, so such a kind of background could be neglected, especially if we compare it with direct mesons yields.

3 Monte Carlo simulation results

For detailed study of the $\vec{p}+\vec{p} \rightarrow \gamma+jet+X$ process we have used the Monte Carlo code SPHINX [24] which is 'polarized' version of PYTHIA [25]. Jet reconstruction was done by the JETSET-subroutine LUCCELL [25]. This routine defines jets in the two-dimensional (η, ϕ) -plane, η being pseudorapidity and ϕ the azimuthal angle. STAR detector covers full space in azimuth and pseudorapidity region $-1 < \eta < 2$.

In order to have segmentation expected at STAR ($\Delta\eta \times \Delta\phi = 0.1 \times 0.1$) we used 30 η -bins and 60 ϕ -bins in our calculation procedure. The values of LUCCELL-subroutine parameters E_{\perp}^{cell} and $R = \sqrt{\Delta\eta^2 + \Delta\phi^2}$ were $E_{\perp}^{cell} = 1.5 \text{ GeV}$ and $R = 0.7$.

The expected resolution of the STAR Electromagnetic Calorimeter $\Delta E/E \simeq 0.16/\sqrt{E}$ was also taken into account [26]. To obtain total rates ($Rate = \sigma \cdot L$) of $\gamma + jet$ events at STAR we taken into account designed integrated luminosity at RHIC: $L = 320 \text{ pb}^{-1}$ at $\sqrt{s} = 200 \text{ GeV}$. The expected values of polarization of proton beams at RHIC ($P_{b1} = P_{b2} = P = 0.7$) were also used in the analysis.

All of the SPHINX calculations were done with a cut on the partonic transverse momentum $p_T > 10 \text{ GeV}/c$. The simulations include initial-state radiation, final-state radiation, fragmentation and particle decay effects.

3.1 Identification of $\gamma + jet$ events and background reduction

After generating the signal event sample we employ the following cuts for reconstruction of candidate $\gamma + jet$ event:

- there is exactly 1 reconstructed jet with $-0.3 < \eta_{jet} < 1.3$, $E_T^{jet} > 10 \text{ GeV}$
- and there is a 1 photon satisfying $-1 < \eta_{\gamma} < 2$, $p_T^{\gamma} > 10 \text{ GeV}/c$.

We would like to note that study of the background enter at this level of the analysis. The direct meson background was simulated by using all possible $2 \rightarrow 2$ partonic hard scattering processes. The event is treated as a candidate direct photon event if there is a high p_T ($p_T > 10 \text{ GeV}/c$) neutral meson (π^0, η) in coincidence with the 1 reconstructed jet ($E_T^{jet} > 10 \text{ GeV}$) satisfying the pseudorapidity cuts defined above.

Figure 2 shows the comparison of the *direct meson + jet* to *direct photon + jet* yields at STAR in $\vec{p} - \vec{p}$ collisions at $\sqrt{s} = 200 \text{ GeV}$ as a function of transverse momentum p_T for the spin-dependent parton distribution $\Delta G^{>0}$ [11]. The signal/background ratio is found to be $S/B \simeq 1/10$. As seen from Figure 2 it is necessary to impose additional cuts for background suppression.

In such cases, the so-called 'isolation cuts' method, developed by UA2 Collaboration [27], have been used for meson background suppression. The candidate direct photon was treated as 'isolated' if no other photons or charged particles fall within a cone of radius R_{isol} around the photon. The idea is that direct meson usually has much more particles in its 'neighborhood' than direct photon.

We tried to make more sophisticated algorithm for photon isolation comparing the energy and multiplicities of particles falling within the isolation cone for different values

of R_{isol} . The results are shown in Figure 3. We have used 3 different values of isolation cone radius: $R_{isol} = 0.26$ (UA2 condition), $R_{isol} = 0.5$ and $R_{isol} = 0.7$.

As seen from Figure 3 particles accompanying the direct photon are softer than those for the direct meson. Also, the use of larger cone radius allow better reduction of background without significant loss of signal. So, the conclusion is that the combination of cuts on multiplicity and energy will give better background suppression. Our results show that highest gamma efficiency $P_{\gamma/\gamma}$ and meson rejection $1 - P_{\gamma/\pi^0}$ (here P_{γ/π^0} is meson contamination) values are obtained under following conditions: the isolation cone radius is $R_{isol} = 0.7$ and summed energy of particles (if there are any) around a direct photon candidate must be lower than 1 GeV . In such a case, 90% of mesons were rejected with gamma efficiency $P_{\gamma/\gamma}$ of 88%.

Figure 4 shows comparison of the *direct meson + jet* to *direct photon + jet* yields at STAR in $\vec{p} - \vec{p}$ collisions at $\sqrt{s} = 200 \text{ GeV}$ as a function of transverse momentum p_T for spin-dependent parton distribution $\Delta G^{>0}$ [11] with the isolation cuts imposed.

Additional event-by-event discrimination between single photons and photon pairs (from neutral mesons decays) at STAR is based on measurement of transverse profile of the electromagnetic shower in Shower Maximum Detector (SMD). It is expected that this approach will rejects $\simeq 80\%$ of photon pairs from meson decays with single gamma efficiency of $\simeq 80\%$ [28, 29, 30].

Figure 5 shows comparison of the *direct meson + jet* to *direct photon + jet* yields at STAR in $\vec{p} - \vec{p}$ collisions at $\sqrt{s} = 200 \text{ GeV}$ as a function of transverse momentum p_T for spin-dependent parton distribution $\Delta G^{>0}$ [11], after the additional *meson*/ γ discrimination with the help of Shower Maximum Detector.

Finally, we can conclude that only combination of isolation cuts and *meson*/ γ discrimination with the help of SMD will be able to reduce the background in the whole p_T region of interest for measuring of double-spin asymmetry A_{LL} and extracting of $\Delta G(x)$ at STAR.

3.2 Asymmetry of $\gamma + jet$ production

In Monte Carlo simulations, the double spin asymmetry is defined through the difference of cross-sections (numbers of $\gamma + jet$ events) for antiparallel ($\uparrow\downarrow$) and parallel ($\uparrow\uparrow$) spins of colliding protons:

$$A_{LL} = \frac{\sigma^{\uparrow\downarrow} - \sigma^{\uparrow\uparrow}}{\sigma^{\uparrow\downarrow} + \sigma^{\uparrow\uparrow}} = \frac{1}{P_{b1}P_{b2}} \frac{N_{\gamma+jet}^{\uparrow\downarrow} - N_{\gamma+jet}^{\uparrow\uparrow}}{N_{\gamma+jet}^{\uparrow\downarrow} + N_{\gamma+jet}^{\uparrow\uparrow}}, \quad (1)$$

with the statistical error:

$$\delta A_{LL} = \frac{1}{P_{b1}P_{b2}} \sqrt{\frac{1 - (P_{b1}P_{b2}A_{LL})^2}{N_{\gamma+jet}^{\uparrow\downarrow} + N_{\gamma+jet}^{\uparrow\uparrow}}}, \quad (2)$$

where P_{b1} and P_{b2} are values of the polarization of proton beams. In our case, only the $\gamma + jet$ events that passed all the above cuts were used for calculation of A_{LL} and extraction of $\Delta G(x)$.

Figure 6 shows the asymmetry A_{LL} of $\gamma + jet$ production in polarized pp collisions at $\sqrt{s} = 200$ GeV for 3 different sets of spin-dependent PDF's ($\Delta G^{>0}$ [11], $\Delta G^{<0}$ [11] and [14]) as a function of transverse momentum p_T . The absolute value of A_{LL} increases with p_T for all spin-dependent PDF's used. There is a clear difference in A_{LL} between positive and negative sign of ΔG as well as between PDF's $\Delta G^{>0}$ [11] and [14] in the region $p_T = (10 - 25)$ GeV/c.

3.3 Partonic kinematics reconstruction

The Bjorken x -values of colliding partons is reconstructed by means of measured γ and jet transverse momenta p_T and pseudorapidities:

$$x_1 = \frac{2p_T (e^{\eta_\gamma} + e^{\eta_{jet}})}{\sqrt{s} \cdot 2}, \quad (3)$$

$$x_2 = \frac{2p_T (e^{-\eta_\gamma} + e^{-\eta_{jet}})}{\sqrt{s} \cdot 2}. \quad (4)$$

The usual procedure [28, 31] is to associate the larger of the x_1, x_2 values with the quark

$$x_q = \max[x_1, x_2], \quad (5)$$

and the smaller one with the gluon momentum fraction

$$x_g = \min[x_1, x_2], \quad (6)$$

with additional condition:

$$\max[x_1, x_2] > 0.2. \quad (7)$$

Comparison of the simulated to reconstructed values of the initial-state parton kinematics for the events that passed all above cuts is shown in Figure 7.

3.4 Extraction of $\Delta G(x)$

The main formula for extraction of $\Delta G(x)$ from $\gamma + jet$ coincidence events can be written in the following form [28]:

$$\Delta G(x_g) = \frac{1}{P_{b1}P_{b2} \sum_{i=1}^{N_s} A_{1p}^{DIS}(x_{qi}, Q_i^2) \cdot \hat{a}_{LL}(\cos \theta_i) / G(x_{gi}, Q_i^2)}, \quad (8)$$

where $N_{x_g}^{\uparrow\downarrow}$ and $N_{x_g}^{\uparrow\uparrow}$ are number of $\gamma + jet$ events for reconstructed value of gluon momentum fraction x_g , for antiparallel ($\uparrow\downarrow$) and parallel ($\uparrow\uparrow$) spins of colliding protons, respectively and $N_s = N_{x_g}^{\uparrow\downarrow} + N_{x_g}^{\uparrow\uparrow}$. Here $\hat{a}_{LL}(\cos \theta_i)$ is the partonic spin-correlation parameter for $qg \rightarrow q\gamma$ process, θ_i being the scattering angle in the partonic center-of-mass (pCM) system. Assuming collinear partonic collisions, the absolute value of $\cos \theta_i$ can be obtained as:

$$\cos \theta_i = \tanh(\pm \eta_i), \quad (9)$$

where

$$\eta_i = \pm \frac{1}{2}(\eta_\gamma - \eta_{jet}). \quad (10)$$

The value of the partonic spin-correlation parameter $\hat{a}_{LL}(\cos\theta_i)$ can be calculated in the LO pQCD [34] and for $qg \rightarrow q\gamma$ process we have:

$$\hat{a}_{LL} = \frac{\hat{s}^2 - \hat{u}^2}{\hat{s}^2 + \hat{u}^2}, \quad (11)$$

where \hat{s} and \hat{u} are the Mandelstam variables for the hard scattering:

$$\hat{s} = x_1 x_2 s, \quad (12)$$

$$\hat{u} = -\frac{\hat{s}}{2}(1 + \cos\theta_i). \quad (13)$$

The factor $A_{1p}^{DIS}(x_{qi}, Q_i^2)$ is a parameterization of the A_1 structure function for the proton obtained by fitting the results of polarized DIS experiments. The value x_{qi} is the quark momentum fraction and Q_i^2 is momentum transfer scale, assumed to be $Q_i^2 = p_T^2/2$. For the calculations done here, we used the following parameterization of A_{1p}^{DIS} [32]:

$$A_{1p}^{DIS}(x_{qi}, Q_i^2) \sim A_{1p}^{DIS}(x_{qi}) = 0.01902 + x_{qi}^{-0.01163}(1 - e^{-1.845x_{qi}}). \quad (14)$$

The parameterization of unpolarized gluon structure function $G(x_{gi}, Q_i^2)$, evaluated at reconstructed value of x_g and evolved to the value of Q_i^2 , was taken from [33].

The results of extraction procedure for spin-dependent parton distribution $\Delta G^{>0}$ [11] at colliding energy of $\sqrt{s} = 200 \text{ GeV}$ is shown in Figure 8. In order to discuss the quality of extraction procedure, we show in Figure 8 the comparison of the input polarized gluon distribution to values extracted from the simulated data as a function of the reconstructed x_{gluon} . The input polarized gluon distribution is evolved to the most probable value $Q^2 = 50 \text{ (GeV/c)}^2$.

In general, theoretical input and the values extracted from the data agree very well. The agreement with results obtained in [6] is also reasonable. The systematic discrepancy for $x_{gluon} < 0.08$ reflects the ambiguity in assigning $x_{1(2)}$ values to gluon (quark) in the small x region and ambiguity in the choice of the sign for $\cos\theta_i$. Also, the behavior of extracted polarized gluon distribution at higher x -values reflects the role of condition (7) and results in relatively small change of the shape of the distribution for $x_{gluon} > 0.2$. Nevertheless, this result shows that $\Delta G(x)$ can be extracted at STAR from the measurements of $\gamma + jet$ production in $\vec{p} - \vec{p}$ collisions. At $\sqrt{s} = 200 \text{ GeV}$, STAR detector will give us the full information about $\Delta G(x)$ in the region $x_{gluon} = (0.03 - 0.3)$.

Figure 9 shows reconstructed values of $x\Delta G(x)$ versus reconstructed values of x_{gluon} for 3 different sets of spin-dependent PDF's ($\Delta G^{>0}$ [11], $\Delta G^{<0}$ [11] and [14]). One can see that measurements at STAR will be able to discriminate between scenarios with positive and negative sign of ΔG . In the case of positive sign of ΔG , extraction of $\Delta G(x)$ at $\sqrt{s} = 200 \text{ GeV}$ will give us possibility to distinguish between theoretical spin-dependent PDF's $\Delta G^{>0}$ [11] and [14] in the region $x_{gluon} = (0.03 - 0.2)$.

4 Conclusions

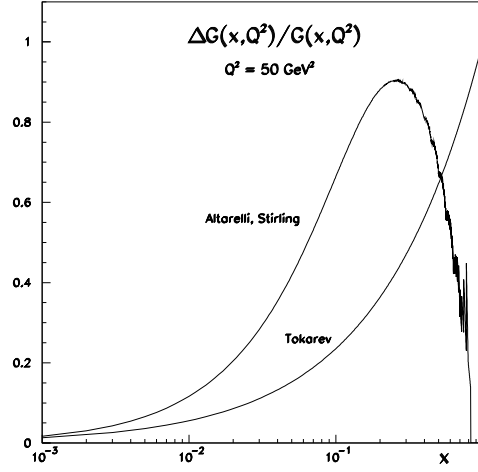
The $\gamma + jet$ production in $\vec{p} - \vec{p}$ collisions at RHIC energies was studied. Double-spin asymmetry A_{LL} of the process is calculated by using Monte Carlo code SPHINX taking into account parameters of the STAR detector. Special attention was paid on the procedure for suppression of meson background. The algorithm for isolation of direct gamma based on 'isolation cuts' method was developed. A procedure for extraction of $\Delta G(x)$ from simulated data sample was described in detail. The obtained results show that highest gamma efficiency and meson rejection values are obtained under following conditions: the isolation cone radius is $R_{isol} = 0.7$ and summed energy of particles (if there are any) around a direct photon candidate must be lower than 1 GeV. In such a case, 90% of mesons were rejected with gamma efficiency of 88%. Also, we concluded that only combination of isolation cuts and $meson/\gamma$ discrimination with the help of Shower Maximum Detector will be able to reduce the background in the whole p_T region of interest for measuring of double-spin asymmetry A_{LL} and extracting of the spin-dependent gluon distribution $\Delta G(x)$ in the region $x_{gluon} = (0.03, 0.3)$ at $\sqrt{s} = 200$ GeV at STAR.

Thus, the obtained results allow us to hope that direct experimental information on a sign of the spin-dependent gluon distribution will give constraints on the quark and gluon distributions and to clarify a role of quark and gluon orbital momenta in proton's spin composition [35].

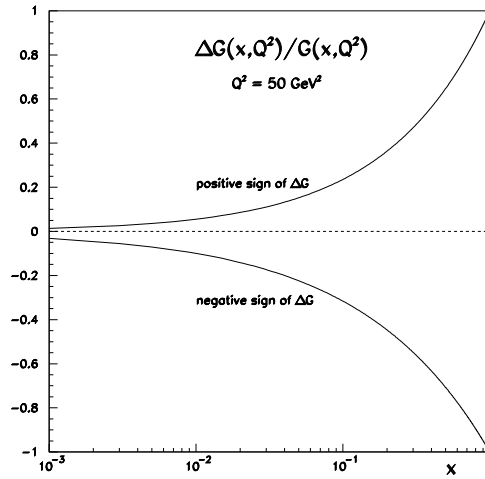
References

- [1] RSC Collaboration, Proposal on Spin Physics using the RHIC Polarized Collider, August 1992.
- [2] G.Bunce et al., Particle World, vol.3, (1992) 1.
- [3] G.Bunce, N.Saito, J.Soffer, and W. Vogelsang, Prospects for SPIN Physics at RHIC, RIKEN-AF-NP-360, July 2000.
- [4] G. P. Škoro, M.V. Tokarev, Nuov. Cim. **A111** (1998) 353.
- [5] G. P. Škoro, M. Zupan, M.V. Tokarev, Nuov. Cim. **A112** (1999) 809.
- [6] L.S. Bland, hep-ex/0002061.
- [7] M. Gluck, E. Reya, M. Stratmann, W. Vogelsang, Phys. Rev. **D53** (1996) 4775; T. Gehrmann, W.J. Stirling, Phys. Rev. **D53** (1996) 6100; G. Altarelli, R.D. Ball, S. Forte, G. Ridolfi, Nucl. Phys. **B496** (1997) 337; E. Leader, A.V. Sidorov, D.B. Stamenov, Phys. Rev. **D58** (1998) 114028.
- [8] H.Y. Cheng, hep-ph/0002157(v2).
- [9] R.D.Ball, S.Forte, G.Ridolfi, Preprint CERN-TH/95-266, 1995.
- [10] D.K. Ghosh, S. Gupta, D. Indumathi, hep-ph/0001287.

- [11] M.V.Tokarev, Preprint JINR, E2-96-304, Dubna, 1996.
- [12] W.-D.Nowak, A.V.Sidorov, M.V.Tokarev, Nuov. Cim. **A110** (1997) 757.
- [13] The HERMES Collaboration, Ackerstaff K., Phys. Rev. Lett. **84** (2000) 2584.
- [14] G.Altarelli, W. J. Stirling, Particle World, vol.1, (1989) p.40.
- [15] The EMC Collaboration, J.Ashman et al., Phys. Lett. **B206** (1988) 364; Nucl. Phys. **B328** (1998) 1.
- [16] The SMC Collaboration, B. Adeva et al., Phys. Rev. **D58** (1998) 112001.
- [17] The E142 Collaboration, P.L. Anthony et al., Phys. Rev. **D54** (1996) 6620.
- [18] The E143 Collaboration, K. Abe et al., Phys. Rev. **D58** (1998) 1120003.
- [19] The E154 Collaboration, K. Abe et al., Phys. Rev. Lett. **79** (1997) 26.
- [20] The E155 Collaboration, P.L. Anthony et al., Phys. Lett. **B463** (1999) 339.
- [21] The HERMES Collaboration, K. Ackerstaff et al., Phys. Lett. **B404 79** (1997) 383.
- [22] The HERMES Collaboration, A. Airapetian et al., Phys. Lett. **B442** (1998) 484.
- [23] W.-D.Nowak, A.V.Sidorov, M.V.Tokarev, In: Proc. International workshop SPIN'97, July 7-12, 1997, Dubna.
- [24] S. Gullenstern et al., Nucl. Phys. **A560** (1993) 494; S. Gullenstern et al., Computer Physics Commun. **87** (1995) 416.
- [25] T.Sjostrand, Computer Physics Commun. **82** (1994) 74.
- [26] T.J. Le Compte, STAR Note 264 (1996).
- [27] J. Alitti et al., Phys. Lett. **B299** (1993) 174.
- [28] S.E.Vigdor, Proc. of 13th Inter. Symp. on High Energy Spin Physics, World Scientific (1999) p. 151.
- [29] L.C. Bland et al., An Endcap Electromagnetic Calorimeter for STAR: Conceptual Design Report, STAR Note 401 (1999).
- [30] Technical Design Report for the Barrel EMC in STAR (1998)
- [31] S. Gullenstern et al., Phys. Rev. **D51** (1995) 3305.
- [32] N. Gagunashvili et al., Nucl. Instr. Meth **A412** (1998) 146.
- [33] M. Gluck, E. Reya, A. Vogt, Z. Phys. **C48** (1990) 471.
- [34] C. Bourrely, J. Soffer, F. M. Renard, P. Taxil, Phys. Rep. **177** (1989) 319.
- [35] R.L. Jaffe, hep-ph/0008038.



a)



b)

Figure 1

The ratio $\Delta G(x, Q^2)/G(x, Q^2)$ of polarized and unpolarized gluon distributions as a function of x for two different parameterizations (a) $\Delta G^{>0}$ [11], [14] and (b) $\Delta G^{>0}$ [11], $\Delta G^{<0}$ [11] at $Q^2=50 \text{ GeV}^2$.

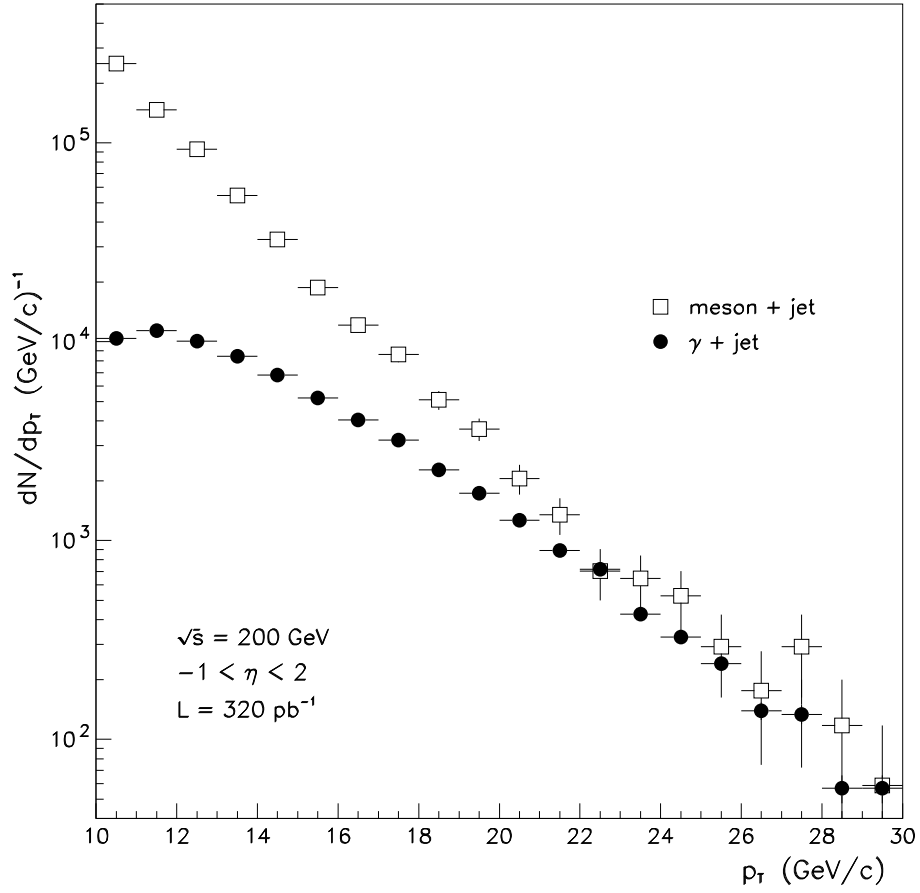


Figure 2.

Comparison of the *direct meson + jet* to *direct photon + jet* yields at STAR in $\vec{p} - \vec{p}$ collisions at $\sqrt{s} = 200 \text{ GeV}$ as a function of transverse momentum p_T for spin-dependent parton distribution $\Delta G^{>0}$ [11].

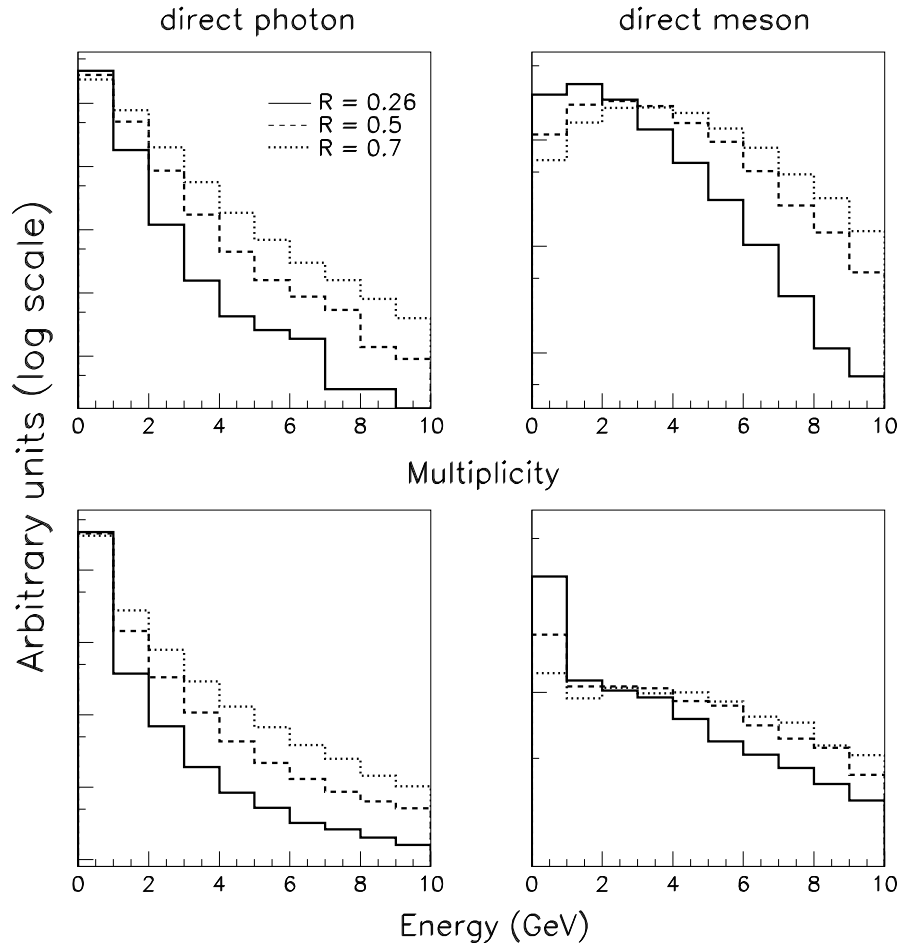


Figure 3.

The multiplicity and summed energy distributions of particles falling within an isolation cone of radius R around a direct photon (left column) or a direct meson (right column).

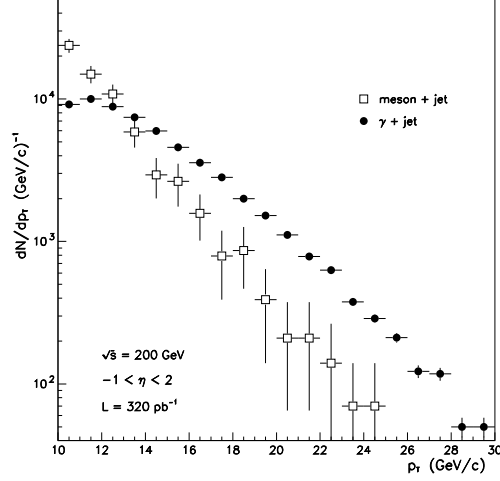


Figure 4.

Comparison of the *direct meson + jet* to *direct photon + jet* yields at STAR in $\vec{p} - \vec{p}$ collisions at $\sqrt{s} = 200 \text{ GeV}$ as a function of transverse momentum p_T for spin-dependent parton distribution $\Delta G^{>0}$ [11], with the isolation cuts imposed (see text).

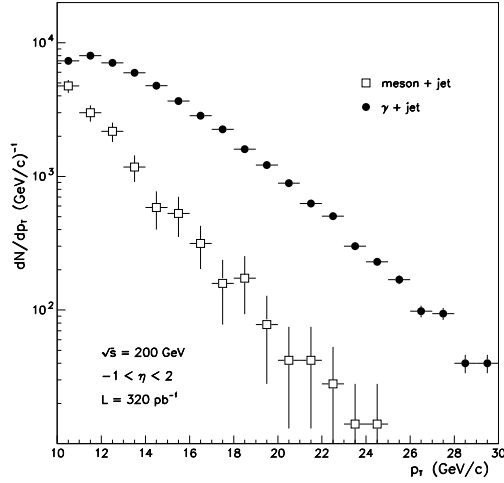


Figure 5.

Comparison of the *direct meson + jet* to *direct photon + jet* yields at STAR in $\vec{p} - \vec{p}$ collisions at $\sqrt{s} = 200 \text{ GeV}$ as a function of transverse momentum p_T for spin-dependent parton distribution $\Delta G^{>0}$ [11], after the additional *meson*/ γ discrimination with the help of Shower Maximum Detector.

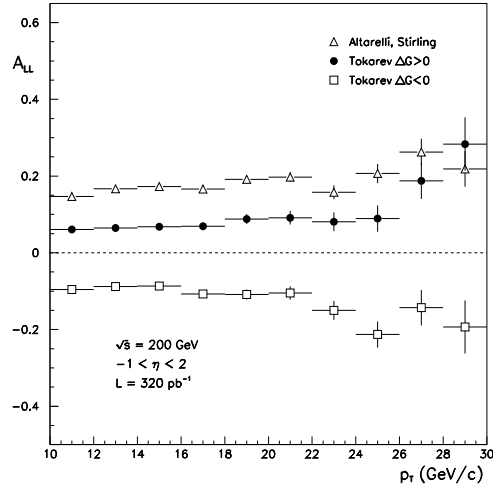


Figure 6.

Asymmetry A_{LL} of $\gamma + jet$ production in polarised pp collisions at $\sqrt{s} = 200$ GeV for 3 different sets of spin-dependent PDF's ($\Delta G^{>0}$ [11], $\Delta G^{<0}$ [11] and [14]) as a function of transverse momentum p_T . The errors indicated are statistical only, based on the expected luminosity of RHIC and the properties of the STAR detector.

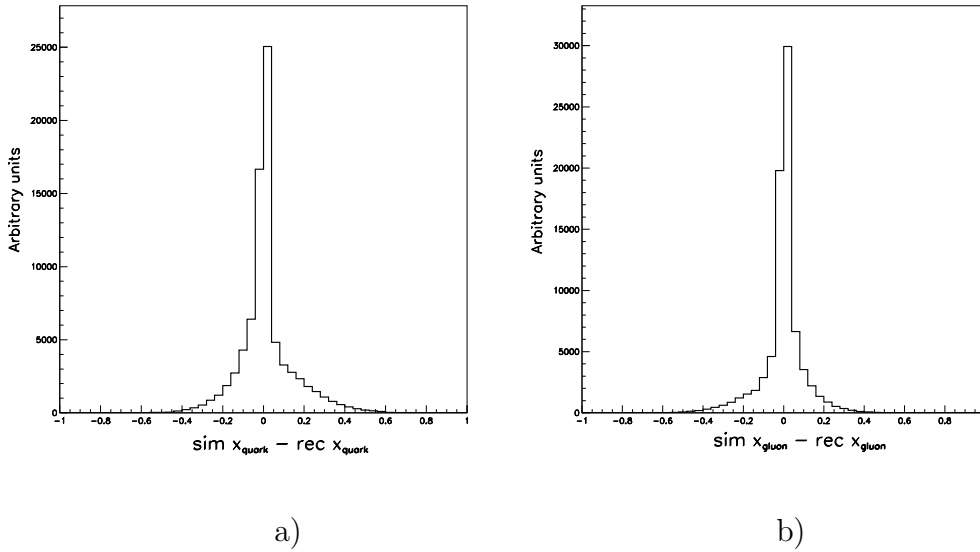


Figure 7. Comparison of the simulated to reconstructed values of the initial-state parton kinematics.

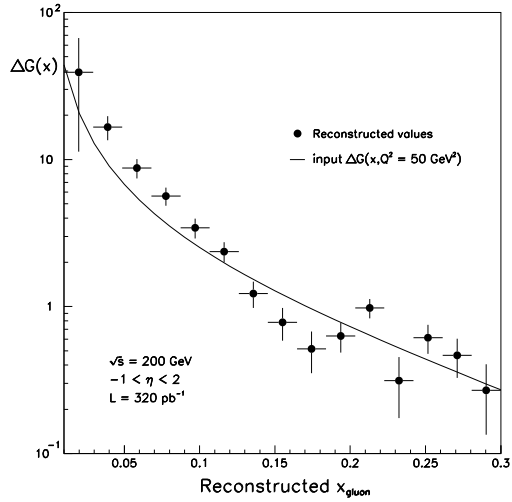


Figure 8.

Comparison of the input polarized gluon distribution (line) $\Delta G(x)$ to values extracted from the simulated data (points) as a function of the reconstructed x_{gluon} . The results are obtained for spin-dependent parton distribution $\Delta G^{>0}$ [11] at colliding energy of $\sqrt{s} = 200 \text{ GeV}$.

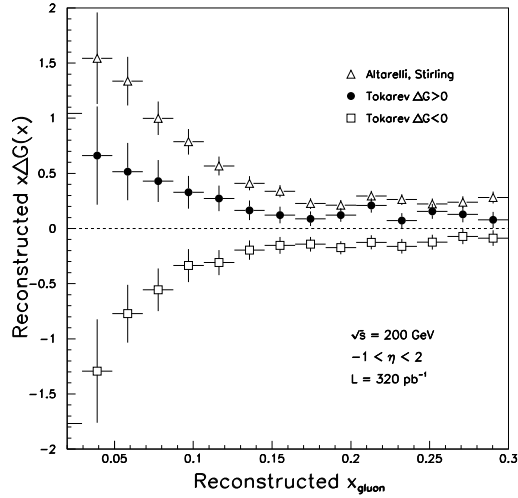


Figure 9.

Reconstructed values of $x\Delta G(x)$ versus reconstructed values of x_{gluon} for 3 different sets of spin-dependent PDF's ($\Delta G^{>0}$ [11], $\Delta G^{<0}$ [11] and [14]).